Propagation properties of the terahertz waveguide using a metallic nanoslit narrower than skin depth

Jie Yang (杨 洁)*, Gongwei Lin (林功伟), Yueping Niu (钮月萍), Yihong Qi (祁义红), Fengxue Zhou (周凤雪), and Shangqing Gong (龚尚庆)

Department of Physics, East China University of Science and Technology, Shanghai 200237, China
**Corresponding author: yangjie7898@ecust.edu.cn*

Received March 10, 2016; accepted April 22, 2016; posted online June 1, 2016

A terahertz (THz) waveguide using a metallic nanoslit whose width is much smaller than the skin depth is analytically investigated. By taking some important physical properties into account, we derive a simple, yet accurate, expression for the effective index. We also study the changes in modal field and the attenuation coefficient in the whole THz region, and find some interesting physical properties. Finally, we verify that these theoretical analyses coincide with the rigorous numerical simulations. This research can be useful for various applications of THz waveguides made of metallic nanoslits.

OCIS codes: 240.6680, 230.7370, 260.3090, 260.3910.
doi: 10.3788/COL201614.072401.

Rapid advances in laser technology have promoted various techniques for the detection and generation of terahertz (THz) radiation, which has shown potential applications in many fields, e.g., in imaging, sensing, and spectroscopy[1–3]. Among this research, powerful THz waveguides have attracted more and more interest[4–21]. It was first proposed by Wang and Mittleman that THz waves can effectively propagate on a simple metal wire[4]. Cao *et al.* quickly demonstrated that the waveguide effect mainly comes from the zeroth-order azimuthally polarized surface plasmon polaritons (SPPs)[5]. Subsequently, various SPP waveguides have also been proposed, such as a channel waveguide[22,23], dielectric-loaded SPP waveguide[24], and hybrid SPP waveguide[25–27]. Most of these SPP waveguides work atsubwavelength scales. As we all know, skin depth is a very important length scale for plasmonics in the THz wave range and other low-frequency radiation[28]. Seo *et al.* demonstrated that the enhancement of a THz electric field inside a slit of width around 30000 times smaller than the wavelength is about 10^5[29]. It was quickly pointed out that the highlight of the work of Seo *et al.* is that they considered a previously unexplored regime in which the skin depth, which is a measure of how quickly the fields decay inside the metal, is larger than both the film thickness and slit width[30]. In spite of that, the results have been applied to many aspects. Up until now, the topics of a THz plasmon of a metallic slit waveguide with sub-skin-depth width have been rarely touched[31]. The propagation properties of a THz waveguide using a metallic nanoslit narrower than the skin depth have not been very clear, to the best of our knowledge.

In this Letter, we shall derive a simple and explicit analytical expression to describe the propagation properties of the THz plasmon of the metallic nanoslit with sub-skin-depth width. The derivation is based on the property of the huge relative permittivity of nonmagnetic metals in the spectral region of the THz wave, and the fact that the width of a nanoslit is much smaller than the skin depth. The broad validity range and the high precision of the analytic expression shall also be tested. It is shown that for all 11 tested nonmagnetic metals mentioned in Ref. [32], in the whole THz radiation region, and with the width ranging from 1 to 10 mm, the relative deviation for the effective index is always smaller than 5%. From the explicit analytical expression, we shall easily find that the propagation properties of this kind of THz waveguide are closely related to the product of the complex wave number of the metal and the width of the metallic slit. We shall also study the changes of modal field and the attenuation coefficient in the whole THz region, and get some interesting physical properties. Specifically, we find that the modal field permeates the metal in a broad region relative to the width of a nanoslit when the width of the metal slit is smaller than the skin depth. Finally, all these analytical conclusions shall be verified with rigorous numerical simulations.

For a flat metal-dielectric interface, as we all know, there is a bound electromagnetic state that is called SPPs[33]. It has two electric field components E_x and E_z, and one magnetic field component H_y. The only magnetic field component H_y denotes the TM polarization. Now we consider metallic slit is surrounded by air, and the width of the slit is w, which is shown in Fig. 1.

For the TM polarization of a nonmagnetic metal, we can obtain the following normalized expressions for the magnetic field component H_y for three regions in Fig. 1,

$$H_y = \exp(\kappa_m k_0 (x + w/2)), \qquad x \le -\frac{w}{2}, \tag{1}$$

$$H_y = \exp(-\kappa_m k_0 (x - w/2)), \qquad x \ge \frac{w}{2}, \tag{2}$$

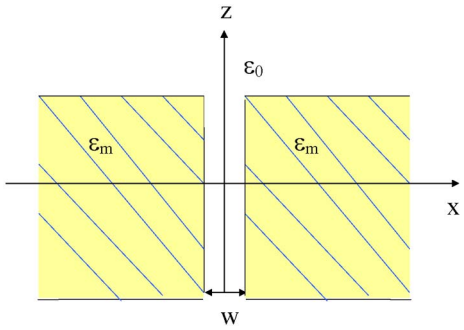

Fig. 1. Schematic of the metallic nanoslit.

$$H_y = a[\exp(-\kappa_a k_0(x + w/2)) + \exp(\kappa_a k_0(x - w/2))] - w/2 \le x \le w/2, \quad (3)$$

where $\kappa_m = [(n_{\text{eff}})^2 - \varepsilon_m]^{1/2}$, $\kappa_a = [(n_{\text{eff}})^2 - 1]^{1/2}$, ε_m is the relative permittivity of the metal, and n_{eff} denotes the effective index of the eigenmode. $k_0 = 2\pi/\lambda_0$, where k_0 and λ_0 denote the wave number in free space and wavelength, respectively. By using Maxwell's equations[34], we can further get two other field components for E_z and E_x. Then, based on the continuities of E_z and H_y at the interface, the following eigen equation can be obtained[35]:

$$\frac{\kappa_m}{\varepsilon_m} + \kappa_a \frac{1 - \exp(-k_0 \kappa_a w)}{1 + \exp(-k_0 \kappa_a w)} = 0. \quad (4)$$

Although n_{eff} is a vital parameter for the Plasmon, it is hidden in Eq. (4) and difficult to work out. So an approximate expression for the effective index n_{eff} is welcome. Using the property $|n_{\text{eff}}^2| \ll |\varepsilon_m|$, one can get $\kappa_m \approx (-\varepsilon_m)^{1/2}$. In addition, the relation $(1 - \exp(-k_0 \kappa_a w))/(1 + \exp(-k_0 \kappa_a w)) \approx k_0 \kappa_a w/2$ always holds when the width w is small. Applying these two approximations into Eq. (4), we can further obtain a simple approximate expression κ_{aa} as follows:

$$\kappa_{aa} = \sqrt{\frac{2}{k_0 w \sqrt{-\varepsilon_m}}}. \quad (5)$$

The corresponding approximate value $n_{\text{eff}a}$ can be further obtained from the relation

$$n_{\text{eff}a} = \sqrt{\kappa_{aa}^2 + 1}. \quad (6)$$

Here our expression is extremely simple but with clear physical significance and high precision because that we use the property of the huge relative permittivity of nonmagnetic metal in the whole THz radiation region. As the propagation properties of the THz plasmons of metal slit working in the sub-skin-depth region, κ_a is also exclusively dependent on the product of $k_0 w(-\varepsilon_m)^{1/2} = jkw$, where the wave number $k = \varepsilon_m^{1/2} k_0$, is the complex wave number[13]. Accordingly, we can draw an important conclusion that the main propagation properties of the THz plasmons of metal slit with the sub-skin-depth width are in close relation to the product of the complex wave number k of the metal and the width w of the metallic slit.

In the following, we shall carefully test the capability of the above analytical expression. The approximate values and the exact values are compared in the width ranging from 1 to 10 mm. We take the metal copper for example, and the frequency is chosen to be 0.5 THz (i.e., $\lambda_0 = 0.6$ mm). The corresponding relative permittivity is $\varepsilon_m = -6.3 \times 10^5 + j2.77 \times 10^6$ according to a fitted Drude formula for copper[32]. We show the approximate values $n_{\text{eff}a}$ and the exact values n_{eff} in Fig. 2(a). And the relative deviations for the real part $n_{\text{eff}a}$ and the imaginary part of n_{eff} are exhibited in Fig. 2(b). The maximum relative deviation of the effective index n_{eff} is smaller than 2% in the considered width range as shown in Fig. 2(b). It should be pointed out that the width $w = 10$ mm is already far larger than the skin depth δ, which is 72.5 nm according to the definition of the skin depth $\delta = \lambda_0/[2\pi \,\text{Im}(\varepsilon_m^{1/2})]$.

It should be pointed out that both of the real and imaginary parts of n_{eff} increase with the decreasing of the slit width. This phenomenon can be explained by the interaction between the SPPs on the two sides of the metal slit. For the wide slit, the coupling between both SPPs on the two sides is weak and can be neglected, so the values of n_{eff} can be simply approximated to that on a single semi-infinite dielectric/metal interface. When the width of the slit is small, the coupling between both SPPs on the two sides cannot be neglected anymore. The increased coupling between both SPPs induces the overlaps of the mode fields and results in the strong confinement of the electromagnetic field and a strong increase in the dispersion and loss, which are represented by the increasing of n_{eff} with the decreasing of slit width.

The applicability of the approximate formula for $n_{\text{eff}a}$ for other nonmagnetic metals mentioned in Ref. [32] is also

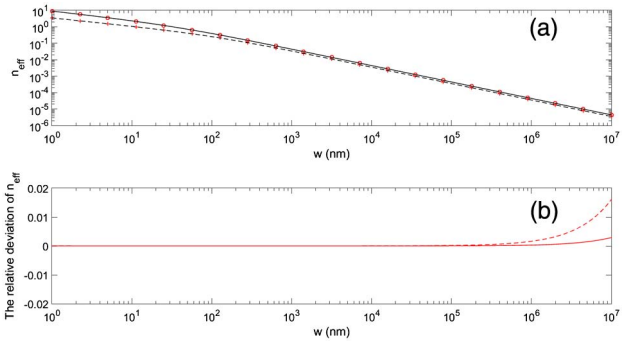

Fig. 2. (a) Comparison between the exact values n_{eff} and the rough values $n_{\text{eff}a}$, for copper at 0.5 THz. The black curves are the rough solutions $n_{\text{eff}a}$ and the red curves denote the exact values n_{eff}. The solid curves are $\text{Re}(n_{\text{eff}a}) - 1$ and the "o" signs represent $\text{Re}(n_{\text{eff}}) - 1$. The dashed curves are $\text{Im}(n_{\text{eff}a})$ and the "+" signs show $\text{Im}(n_{\text{eff}})$. (b) The relative deviation of $n_{\text{eff}a}$. The solid curve is the relative deviation of $\text{Re}(n_{\text{eff}a}) - 1$, and the dashed curve represents the relative deviation of $\text{Im}(n_{\text{eff}a})$.

tested. It is shown that Eq. (6) also performs well for all other nonmagnetic metals of Al, Ag, Au, Mo, W, Pd, Ti, Pb, Pt, and V. The maximum relative deviation of the effective index n_{eff} is always less than 5% for all 11 tested nonmagnetic metals in the whole spectral region of THz radiation with the width ranging from 1 to 10 mm. Therefore, we can see the broad validity range of the approximate formula for $n_{\text{eff}a}$.

As we all know, the attenuation coefficient α is related to the imaginary part of the effective index by the relation $\alpha = k_0\,\text{Im}(n_{\text{eff}})$. Based on the exact value of n_{eff} and the approximate value $n_{\text{eff}a}$, we also compare the exact values and the calculated values of the attenuation coefficient in the width ranging from 1 to 10 mm, as shown in Fig. 3. The metal and the frequency are chosen to be the same as those in Fig. 2. From Fig. 3, we can see that the calculated values and the exact values agree well, which furthermore proves the accuracy of the approximate formula for $n_{\text{eff}a}$. In addition, we can also see that the values of the attenuation coefficient increase with the decrease in the width of metal slit.

To get an intuitive impression on the size of the modal field, we calculate the normalized magnetic field H_y for three different values of w. The metal and the frequency are both chosen as noted above. For comparison, $w = 5$, 50, and 500 nm are chosen as three different metal slit widths. The scope of radial coordinate x/w is set as $-3 \le x/w \le 3$. The corresponding results are shown in Fig. 4. From it, one can see that the decay of the modal field decreases with the increase in the width of the nanoslit. From Fig. 4(a), we find that H_y fields is almost invariant in the chosen region, which is quite different from that of the metallic slit with a broad width, as shown in Fig. 4(c).

In conclusion, we establish a simple yet accurate expression for a THz plasmon of a metallic nanoslit with a sub-skin-depth width. This formula performs well for all 11 of the tested kinds of nonmagnetic metals in the whole spectral region of THz radiation with the wide slit width ranging from 1 to 10 mm. The main propagation

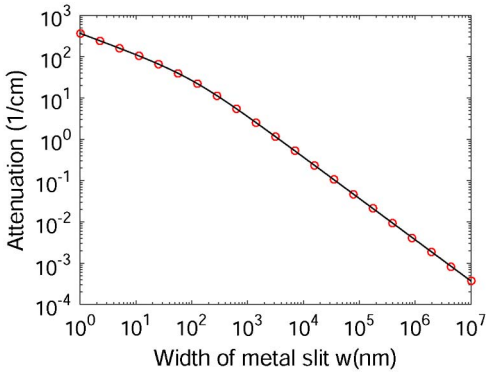

Fig. 3. Comparison between the exact values and the calculated values of the attenuation coefficient in the width ranging from 1 to 10 mm for copper and 0.5 THz. The red curves are the exact values, and the "o" signs show the calculated values.

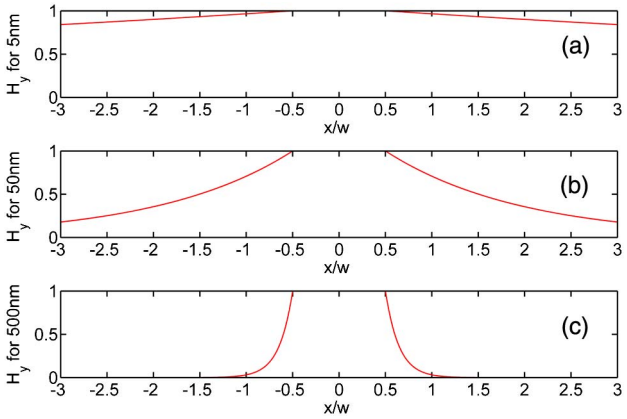

Fig. 4. Magnetic field H_y for metal copper and 0.5 THz. (a) The case for the metallic slit with width of 5 nm. (b) The case for the width of 50 nm. (c) The case for the width of 500 nm.

properties are found to be in close relation to the product of the complex wave number of the metal and the width of the metallic slit. Furthermore, when the width of the metallic slit is smaller than the skin depth, the modal field permeates the metal in a broad region relative to the width of the nanoslit. These research results can be useful for the various applications of a THz slit waveguide with sub-skin-depth width.

We sincerely thank Prof. Qing Cao for the many helpful discussions. This work was supported by the National Natural Sciences Foundation of China under Grants Nos. 11347155, 91321101, 11474092, 11274112, and 11204080.

References

1. C. Jansen, S. Wietzke, O. Peters, M. Scheller, N. Vieweg, M. Salhi, N. Krumbholz, C. Jördens, T. Hochrein, and M. Koch, Appl. Opt. **49**, E48 (2010).
2. C. Debus and P. H. Bolivar, Appl. Phys. Lett. **91**, 184102 (2007).
3. Y. C. Shen, T. Lo, P. F. Taday, B. E. Cole, W. R. Tribe, and M. C. Kemp, Appl. Phys. Lett. **86**, 241116 (2005).
4. K. Wang and D. M. Mittleman, Nature **432**, 376 (2004).
5. Q. Cao and J. Jahns, Opt. Express **13**, 511 (2005).
6. Z. G. Zhong, T. Yan, S. H. Qi, Z. C. Lin, and Y. G. Zhen, Chin. Phys. Lett. **23**, 1456 (2006).
7. M. Wächter, M. I. Nagel, and H. Kurz, Appl. Phys. Lett. **90**, 061111 (2007).
8. J. Yang, Q. Cao, and C. Zhou, Opt. Express **17**, 20806 (2009).
9. A. Ishikawa, S. Zhang, D. A. Genov, G. Bartal, and X. Zhang, Phys. Rev. Lett. **102**, 043904 (2009).
10. P. Tannouri, M. Peccianti, P. L. Lavertu, F. Vidal, and R. Morandotti, Chin. Opt. Lett. **9**, 110013 (2010).
11. J. Gu, Z. Tian, Q. Xing, C. Wang, Y. Li, F. Liu, L. Chai, and C. Wang, Chin. Opt. Lett. **8**, 1057 (2010).
12. J. Yang, Q. Cao, and C. Zhou, J. Opt. Soc. Am. A **27**, 1608 (2010).
13. J. Yang, Q. Cao, and C. Zhou, Opt. Express **18**, 18550 (2010).
14. J. Yang, Y. P. Niu, G. Lin, Y. Qi, and S. Gong, Chin. Opt. Lett. **11**, 082501 (2013).
15. X. Wang, F. Liu, A. Liu, B. Fan, K. Cui, X. Feng, W. Zhang, and Y. Huang, Chin. Opt. Lett. **12**, 010602 (2014).

16. C. Ye, Y. Liu, J. Wang, H. Lv, and Z. Yu, Chin. Opt. Lett. **12**, 092402 (2014).
17. A. M. Lerer, I. V. Donets, G. A. Kalinchenko, and P. V. Makhno, Photon. Res. **2**, 31 (2014).
18. H. Amarloo and S. Safavi-Naeini, J. Opt. Soc. Am. A **32**, 2189 (2015).
19. O. Sydoruk, J. B. Wu, A. Mayorov, C. D. Wood, D. K. Mistry, and J. E. Cunningham, Phys. Rev. B **92**, 195304 (2015).
20. Q. Zhang, C. Tan, C. Hang, and G. Huang, Chin. Opt. Lett. **13**, 082401 (2015).
21. X. Li, J. Song, and J. X. J. Zhang, Opt. Commun. **361**, 130 (2016).
22. S. I. Bozhevolnyi, V. S. Volkov, E. Devaux, J. Y. Laluet, and T. W. Ebbesen, Nature **440**, 508 (2006).
23. B. Wang and G. Wang, Appl. Phys. Lett. **87**, 013107 (2005).
24. J. Grandidier, S. Massenot, G. Colas des Francs, A. Bouhelier, J.-C. Weeber, L. Markey, A. Dereux, J. Renger, M. U. González, and R. Quidant, Phys. Rev. B **78**, 245419 (2008).
25. R. F. Oulton, V. J. Sorger, D. A. Genov, D. Pile, and X. Zhang, Nat. Photon. **2**, 496 (2008).
26. S. H. Nam, A. J. Taylor, and A. Efimov, Opt. Express **17**, 22890 (2009).
27. X. Zhou, T. Zhang, L. Chen, W. Hong, and X. Li, J. Lightwave Technol. **32**, 3597 (2014).
28. A. K. Azad and W. Zhang, Opt. Lett. **30**, 2945 (2005).
29. M. A. Seo, H. R. Park, S. M. Koo, D. J. Park, J. H. Kang, O. K. Suwal, S. S. Choi, P. C. M. Planken, G. S. Park, N. K. Park, Q. H. Park, and D. S. Kim, Nat. Photon. **3**, 152 (2009).
30. L. Martin-Moreno, Nat. Photon. **3**, 131 (2009).
31. A. Novitsky, M. Zaikovskij, R. Malureanu, and A. Lavrinenko, Opt. Commun. **284**, 5495 (2011).
32. M. A. Ordal, R. J. Bell, R. W. Alexander, L. L. Long, and M. R. Querry, Appl. Opt. **24**, 4493 (1985).
33. H. Raether, *Surface Plasmons on Smooth and Rough Surfaces and on Gratings* (Springer, 1988).
34. M. Born and E. Wolf, *Principles of Optics*, 5th ed. (Pergamon Press, 1975).
35. S. Collin, F. Pardo, and J.-L. Pelouard, Opt. Express **15**, 4310 (2007).